Line-of-Sight Guidance for Path Following of Marine Vehicles

Chapter · June 2013

CITATIONS
30

READS
1,913

2 authors:

Anastasios M. Lekkas
Norwegian University of Science and Technology
20 PUBLICATIONS **303** CITATIONS
SEE PROFILE

Thor I. Fossen
Norwegian University of Science and Technology
392 PUBLICATIONS **16,486** CITATIONS
SEE PROFILE

Line-of-Sight Guidance for Path Following of Marine Vehicles

Anastasios M. Lekkas and Thor I. Fossen

Abstract This paper presents an overview of the Line-of-Sight (LOS) guidance law, which is a widely used method for generating heading reference trajectories, for path-following applications of marine vehicles. Due to the fact that these reference trajectories depend also on the form of the path, five path evaluation criteria are discussed. The guidance problem is presented in a constructive manner. First, two 2-D cases are studied, therefore it is assumed that the horizontal-plane motion and the vertical-plane motion are decoupled. The next step is to consider a 3-D path-following scenario for a 5-DOF underwater vehicle where the motions are coupled. The interconnection between the LOS guidance and the heading/pitch controller is explained and a brief overview of depth control methods is given. Moreover, a short review of integral LOS methods in order to compensate for unknown external disturbances is presented and it is shown how course control can circumvent this problem.

1 Introduction

Guidance systems are of utmost importance when considering the performance of aerial, surface and underwater vehicles, regardless of the motion control scenario involved. For more information on control motion scenarios, such as target tracking, path following, path tracking and path maneuvering, the interested reader is referred to [7, 3, 42]. Path-following refers to the case where the control objective

Anastasios M. Lekkas
Department of Engineering Cybernetics, Norwegian University of Science and Technology, NO-7491, Trondheim, Norway, e-mail: anastasios.lekkas@itk.ntnu.no

Thor I. Fossen
Centre for Autonomous Marine Operations and Systems, Department of Engineering Cybernetics, Norwegian University of Science and Technology, NO-7491, Trondheim, Norway, e-mail: fossen@ieee.org

is to converge to and follow a predefined path without involving any requirements pertaining to temporal constraints. In order to achieve this, several guidance laws have been studied and implemented in the past, with the missile community being most likely the oldest and most active one on the field. As a matter of fact, some of the most commonly used approaches by the marine control community have been directly influenced by their missile community counterparts, such as the Line-of-Sight (LOS) guidance, the Pure Pursuit (PP) guidance and the Constant Bearing (CB) guidance. The implementation of the three aforementioned methodologies in the case of autonomous underwater vehicles has been discussed extensively in [6].

The LOS guidance algorithm and its properties have been studied thoroughly in the literature. Frequently, the LOS guidance is considered in connection with the heading autopilot due to the fact that the two systems form together a cascade structure that needs to be stabilized. One of the first efforts of this kind was presented in [21]. In [18], an implementation of the LOS guidance law for straight line path following can be found, whereas in [4] the motion of a particle was considered and the method was implemented for curved path following. A cascaded systems approach was also developed by [2] where the guidance system is interconnected with a sliding mode controller in order to achieve global κ-exponential stability when the desired path is a straight line in 3-D space. The concept of global κ-exponential stability was introduced in [37] and is equivalent to Uniform Global Asymptotic Stability (UGAS) and Uniformly Local Exponential Stability (ULES) combined. All the aforementioned approaches assumed a constant lookahead distance. In general, a small lookahead distance will induce more aggressive steering, hence resulting in reaching the desired path faster, but it might also be the reason for unwanted oscillations around the path. On the other hand, a large lookahead distance results in a smoother steering which prevents unwanted oscillations, but the downside is slower convergence to the path. The idea of combining these behaviors in a complementary manner was investigated in recent works, such as [5],[34],[32] and [27] where the authors discussed and implemented the possibility of using a time-varying lookahead distance. These works, regardless of the theory each one of them was based on, indicated that a time-varying lookahead distance can contribute to converging to the desired path faster while at the same time reducing oscillations around the path.

Although the LOS guidance algorithm is efficient and has a very simple structure, when unknown forces (due to the wind or sea currents, for example) act on the vehicle it is not possible (in the general case) to succeed in accomplishing the motion control task, i.e. to converge to the desired path. A common and reasonable strategy is then to augment the LOS guidance law by adding integral action in order to eliminate any constant offsets induced by the constant, or slow time-varying, environmental forces. In [6] the addition of a simple integrator is discussed, whereas in [1] a more sophisticated approach was followed resulting in a method that avoided the integrator wind-up phenomenon.

This work presents an overview of the lookahead-based LOS guidance law in its conventional form, when implemented for marine applications, and follows a constructive approach. Initially, two uncoupled 3-DOF models are considered, the first pertains to guidance on the horizontal plane and the second pertains to guidance on

the vertical plane. Stability proofs are given in both cases, assuming perfect heading and pitch tracking respectively, and the result shows how the sideslip angle and the angle of attack affect the performance. Next, a more general case in 3-dimensional space is studied. The task is to converge to a straight line which is at a known depth underwater. In this case the horizontal plane LOS guidance system is coupled with the depth controller and the stability analysis is more complicated and it also depends on the type of depth controller used.

In path-following applications, the shape and the properties of the path itself have a great influence on the reference trajectories generated by the LOS algorithm. Therefore, the path-planning problem is directly correlated to the guidance problem. It is often sufficient to design paths that consist of successive straight lines, this selection offers simplicity since the path-tangential angle is constant for each line and it also makes it easier to compensate for constant environmental disturbances, such as winds and ocean currents. Stability proofs can also be more tractable when using straight line paths. On the other hand, such paths result in a non-smooth velocity function and, consequently, curvature, resulting in sudden increases of the cross-track error when switching to the next waypoint. There is a vast literature on the properties of the several path-planning methods and therefore a wide variety of paths to choose from. Depending on the application and the constraints, properties such as curvature continuity or minimum length might be more important to satisfy than others. In this paper, paths based on straight lines are used to demonstrate the efficiency of the LOS guidance. In addition, a section with a discussion on criteria that can help the user evaluate the path candidates is given.

The rest of this paper is organized as follows: Section 2 presents the dynamic model of the vessel. Section 3 discusses five path evaluation criteria than can be considered when making a decision upon which path should be used. In Section 4, the 3-DOF LOS guidance is presented for a vessel navigating on the horizontal, as well as the vertical, plane. Here the two cases are assumed to be uncoupled. In Section 5, a three-dimensional scenario is studied and in this case the horizontal LOS guidance system is coupled with the depth controller. Section 6 deals with guidance under the influence of constant environmental disturbances and reviews two LOS-based methods to tackle the problem. Furthermore, it gives an explanation of why no integral action needs to be added when the course angle, instead of the yaw angle, is controlled. Finally, Section 7 gives a brief summary of the paper.

2 Vehicle Models

This section presents the vessel model and the related assumptions that are considered in this paper. Two reference frames, namely, the *North-East-Down* (NED) coordinate system $\{n\} = (x_n, y_n, z_n)$ and the body-fixed reference frame $\{b\} = (x_b, y_b, z_b)$ will be adopted in this paper to describe the motion, location and orientation of the vehicle. The NED frame is defined as a tangent plane on the surface of the Earth moving with the vehicle and is sufficient for local operations. Its origin is o_n and

the x axis points towards the true *North*, the y axis points towards the true *East* and the z axis points *downwards*, normal to the Earth's surface. The body-fixed frame is moving with the vehicle and its origin o_b coincides with the center of gravity of the vehicle, see also [16, Ch. 2].

2.1 Vehicle Dynamics

Similarly to [2], for the path-following task we can neglect the roll angle, hence for an underactuated autonomous vehicle the following 5-DOF dynamic model can be used:

$$\dot{\eta} = \mathbf{J}(\eta)\nu, \tag{1}$$

$$\mathbf{M}\dot{\nu} + \mathbf{C}(\nu)\nu + \mathbf{D}(\nu)\nu + \mathbf{g}(\eta) = \tau, \tag{2}$$

where $\mathbf{M}$ is the mass and inertia matrix, $\mathbf{C}(\nu)$ is the Coriolis and centripetal matrix, $\mathbf{D}(\nu)$ is the damping matrix, $\mathbf{g}(\eta)$ describes the gravitational and buoyancy forces, and τ includes the control forces and moments.

Accordingly, the generalized position and velocity are recognized as:

$$\eta = (x,\ y,\ z,\ \theta,\ \psi)^{\mathrm{T}},\ \ \nu = (u,\ v,\ w,\ q,\ r)^{\mathrm{T}}, \tag{3}$$

where (x,y,z) is the vehicle's inertial position in Cartesian coordinates, θ is the pitch angle and ψ is the yaw angle. In addition, u is the surge velocity, v is the sway velocity, w is the heave velocity, q is the pitch rate and r is the yaw rate.

2.2 Kinematic Models

There are two kinematics models corresponding to (1) that are common to use. The main difference between them is the incorporation of the effects of ocean currents. The first model considers only absolute velocities and is the following:

$$\dot{x} = u\cos(\psi)\cos(\theta) - v\sin(\psi) + w\cos(\psi)\sin(\theta), \tag{4}$$

$$\dot{y} = u\sin(\psi)\cos(\theta) + v\cos(\psi) + w\sin(\psi)\sin(\theta), \tag{5}$$

$$\dot{z} = -u\sin(\theta) + w\cos(\theta), \tag{6}$$

$$\dot{\theta} = q, \tag{7}$$

$$\dot{\psi} = \frac{1}{\cos(\theta)}r, \quad \cos(\theta) \neq 0. \tag{8}$$

As it is shown in [17], by incorporating relative velocities, the kinematics can be rewritten as:

$$\dot{x} = u_r \cos(\psi)\cos(\theta) - v_r \sin(\psi) + w_r \cos(\psi)\sin(\theta) + u_c^n, \tag{9}$$

$$\dot{y} = u_r \sin(\psi)\cos(\theta) + v_r \cos(\psi) + w_r \sin(\psi)\sin(\theta) + v_c^n, \tag{10}$$

$$\dot{z} = -u_r \sin(\theta) + w_r \cos(\theta) + w_c^n, \tag{11}$$

$$\dot{\theta} = q, \tag{12}$$

$$\dot{\psi} = \frac{1}{\cos(\theta)} r, \quad \cos(\theta) \neq 0. \tag{13}$$

where the relative velocities in surge, sway and heave $(u_r,\ v_r,\ w_r)$ and their absolute velocities counterparts are related as follows:

$$u_r = u - u_c^b,\ \ v_r = v - v_c^b,\ \ w_r = w - w_c^b, \tag{14}$$

with $(u_c^b,\ v_c^b,\ w_c^b)$ denoting the ocean current velocities in the body-fixed frame and $(u_c^n,\ v_c^n,\ w_c^n)$ denoting the ocean current velocities in the NED frame.

It is worth noting that, even in the presence of ocean currents, it can be easily shown that the two kinematic models, (4)–(8) and (9)–(13) are equivalent. However, the overall analysis of the system, including the stability results of the LOS algorithm, can change a lot depending on which one of the two is adopted. The main criterion for choosing either one is the available measurements and what states of the system are controlled. For instance, if Global Navigation Satellite System (GNSS) measurements are available, then the absolute velocities are measured. Consequently, even if ocean current forces are present, it is possible to reduce the uncertainty and simplify the analysis by controlling the course angle and using conventional LOS guidance. For an underwater vehicle with only relative measurements available though, the relative velocities model with yaw control and an augmented LOS guidance law with integral action is is a more fitting option. These issues are discussed in detail in Section 6.

3 Path Planning and Evaluation Criteria

3.1 Introduction

In the case of a path-following motion control scenario, it is important to decide upon the path to be followed before designing and implementing a guidance algorithm, this is commonly known as the path planning task. It is with respect to this path that the guidance reference trajectories will be generated and, depending on the overall task conditions and constraints, these paths can vary a lot. Frequently, the first step is to introduce a given order of fixed points in space, namely the waypoints, and define the desired path as the sum of the successive straight lines that connect these waypoints. This approach, although simple, might not be sufficient for applications that demand high accuracy because the resulting path is not smooth. There is a vast literature pertaining to this issue, as well as other important factors

that arise and affect the performance in each considered case. For some missions, for example, it is critical that the vehicle converges to and stays on the exact path, whereas others are more concerned with finding the minimum length path, and so on. As a consequence, many different solutions have been presented and each one of them satisfies some desired properties that are prioritized.

Dubins showed, for instance, that for a particle with unity speed, the shortest possible path that meets a maximum curvature bound between a starting position with predefined orientation (starting pose) and a finishing position with predefined orientation (finishing pose) consists of at most three pieces, each of which is either a straight line or an arc of a circle of radius $R > 0$ [14]. However, the Dubins methodology does not result in curvature continuous paths due to the fact that a straight line has a curvature $\kappa = 0$, whereas a circle arc has a curvature $\kappa = 1/R$. Hence, there will be a jump in the curvature from 0 to $1/R$ when moving from the straight line to the circle arc. The Euler spirals (also known as clothoids) is an alternative approach that gives curvature continuous paths, but it is also more expensive from a computational point of view because it has an open form solution which includes the calculation of the Fresnel integrals. Other popular alternatives are the Pythagorean Hodographs, first introduced in [15] and the potential field method. For a more detailed and thorough treatment of path planning methods the reader is referred to [40] and [24].

3.2 Path Evaluation Criteria

Given the variety of the methodologies available when it comes to deciding which path is more suitable for an application, it is useful to introduce a few evaluation criteria that can help the user make a more fitting decision. Some of the criteria presented below have been mentioned also in [11].

3.2.1 Path Smoothness

This property is among the most important ones, due to the fact that it is directly related to the vehicle dynamic constraints, hence it has motivated many researchers to investigate new methodologies. Two notions can be used to describe the path smoothness, namely, the parametric continuity and the geometric continuity. The main difference is that parametric continuity refers to both the speed and the orientation with which the parameter propagates through the path, whereas the geometric continuity is not concerned with the parameter speed. Therefore, parametric continuity can be considered as a subset of geometric continuity. More specifically, regarding geometric continuity:

- G^0: all subpaths are connected.
- G^1: the path tangential angle is continuous.
- G^2: the center of curvature is continuous.

Accordingly for parametric continuity:

- C^0: all subpaths are connected.
- C^1: the velocity is continuous.
- C^2: the acceleration (hence, the curvature) is continuous.

A G^1 curve looks identical to a C^1 curve, however the speed magnitude is discontinuous for the G^1 curve. Consequently, for a path-following scenario geometric continuity is equivalent to parametric continuity, but the same is not true for a motion control scenario that includes temporal constraints, such as path-tracking.

3.2.2 Path Length

Following [30, Ch. 3], a regular arc $\mathbf{x} = \mathbf{x}(t)$, $a \leq t \leq b$ is rectifiable and its length can be computed by the integral:

$$s = \int_a^b \left| \frac{d\mathbf{x}}{dt} \right| dt = \int_a^b \sqrt{\left(\frac{dx_1}{dt}\right)^2 + \left(\frac{dx_2}{dt}\right)^2 + \left(\frac{dx_3}{dt}\right)^2}\, dt. \tag{15}$$

In many applications the goal is to design a path that will minimize (15) since this can be associated with arriving to the destination faster, or consuming less energy. However, this is not always true, as it can be demonstrated by the Zermelo navigation problem where the task is to find the trajectory that minimizes the travel time when there is a constant force field (such as a steady current) present. In this case, the straight line is not the optimal path anymore. Moreover, regarding the path length optimality of the Dubins paths, it is worth noting that, depending on the application, it is not always possible to find a Dubins path, as it was shown in [39].

3.2.3 Path Precision

Given a number of waypoints, path precision refers to whether the designed path passes through all the waypoints (interpolating curve) or passes through some of them and comes close to, but without passing through, the rest (approximating curve). Such a property can be important in cases where the vehicle navigates in an area with obstacles that have to be avoided.

3.2.4 Path Tractability

This property is concerned with two main issues: a) if the overall shape of the path is of practical use, and b) what happens in the rest of the path if one of the waypoints changes location. The first branch pertains to any unnecessary zig-zagging or wiggling the path might include between two successive waypoints. This can be the result of satisfying another property, especially a continuous curvature. An exam-

ple is the natural cubic spline, which can give curvature-continuous paths but their overall resulting geometry can often be very unsuitable for vehicle navigation. On the other hand, a monotone cubic spline methodology, such as the one presented in [19], can give paths with a very practical shape, but without preserving curvature continuity at the waypoint locations.

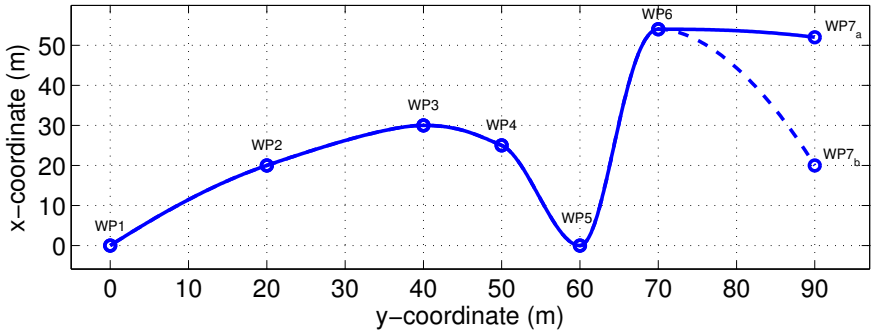

Fig. 1 Local control and monotonicity of the implemented path-planning method are shown. The last waypoint of the initial path has changed, but in a way such that the lines $WP6-WP7_{\mathrm{a}}$ and $WP6-WP7_{\mathrm{b}}$ have slopes of the same sign. This change does not affect the overall shape of the initial path.

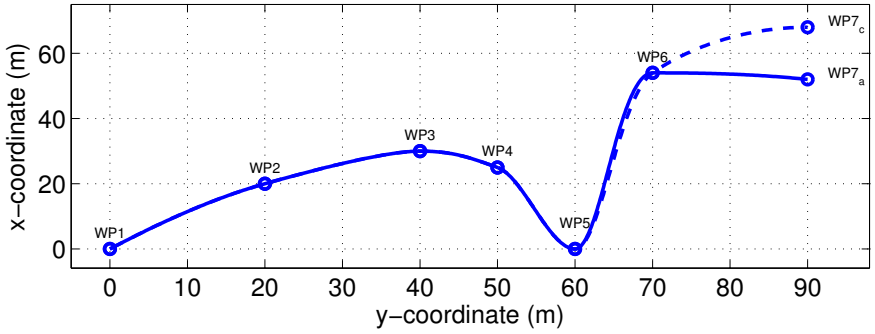

Fig. 2 Partial local control of the monotone CHSI method is shown. In this case the last waypoint of the initial path changes in a way such that the slopes of $WP6-WP7_{\mathrm{a}}$ and $WP6-WP7_{\mathrm{c}}$ have a different sign. This causes a small change at the segment $WP5-WP6$.

The second branch can be of importance in cases where due to updated weather data, for instance, one segment of the path should be avoided and one (or more) waypoint should change location. The question then is what happens to the rest of the path, and especially the part which precedes the newly-assigned waypoint

because this might affect the vessel at its current position. Depending on the result, three different path control behaviors can be distinguished: 1) local control, where it is possible to change a waypoint without affecting the rest of the path, 2) global control, where there will be changes through the whole path, and 3) partial control, where in some cases local control is possible. An example of a local control method is the Cubic Hermite Spline Interpolation (CHSI), while natural cubic splines is a global control method and the monotone CHSI is a partial control method. The latter is demonstrated in Figs. 1-2.

3.2.5 Algorithm Complexity

Naturally, each path planning method is based upon different principles and the involved mathematics might result in algorithms that are computationally more expensive than others. Path planning is a real-time process and, although large vessels should have enough computational power available, the same might not be true for smaller unmanned vehicles with limited power. In dynamic environment with moving obstacles, the path generation algorithm must be able to give feasible solutions within limited time and this can make the task a difficult one if the method is based on open form solutions.

4 LOS Guidance Designs for the Decoupled Horizontal and Vertical Planes

4.1 Introduction

This section deals with path-following in two dimensions by considering two independent and decoupled 3-DOF cases, namely, the horizontal plane guidance and the vertical plane guidance. The former is concerned with generating appropriate heading reference trajectories in order for the vehicle to converge to a straight line on the xy-plane and, similarly, the latter generates pitch reference trajectories in order to converge to a straight line on the xz-plane. For either of them a LOS guidance law that results in a κ-exponentially stable equilibrium point is derived. The reason for studying these decoupled cases is twofold: first, the horizontal plane case is exactly how the problem is stated and tackled for a surface vessel performing path-following, and second, breaking the problem in two parts contributes to presenting a more constructive approach and serves as a smooth transition to the 3-D case. In this section it is assumed that no environmental disturbances are present. Moreover, a discussion on the cascaded system formed by the LOS guidance law and the heading, or pitch, angle controller is included at the end of the section.

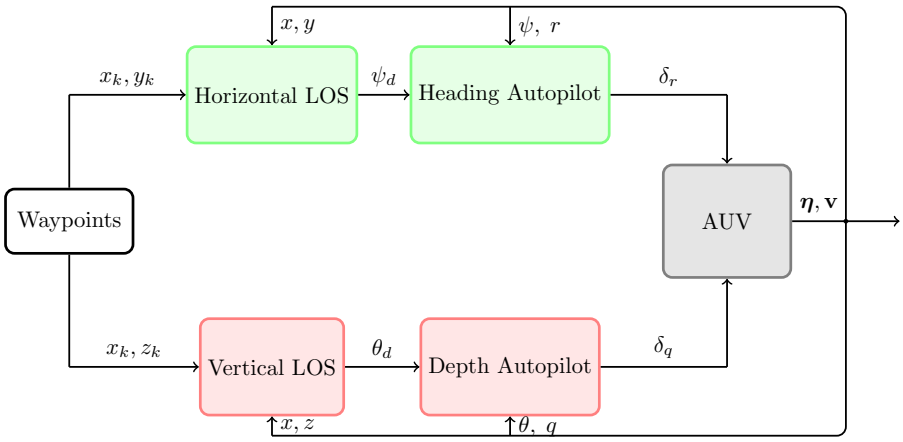

Fig. 3 Block diagram of the decoupled LOS guidance for the horizontal and vertical planes.

4.2 Horizontal-Plane Path Following

In the case of decoupled horizontal plane path-following we assume that $\theta = 0^\circ$, consequently the kinematics equation to be considered is:

$$\dot{x} = u\cos(\psi) - v\sin(\psi), \tag{16}$$
$$\dot{y} = u\sin(\psi) + v\cos(\psi), \tag{17}$$
$$\dot{\psi} = r. \tag{18}$$

The horizontal speed U_h is given by:

$$U_h := \sqrt{u^2 + v^2}, \tag{19}$$

and is assumed to be positive and bounded:

$$U_{h,\min} \leq U_h \leq U_{h,\max},\ \ 0 < U_{h,\min}. \tag{20}$$

From (19)–(20) it is implied that the vessel always has at least a nonzero surge speed. The reason for setting a minimum positive speed $U_{h,\min}$ is related to the stability proof of the LOS guidance and will be explained in Section 4.2.2. The model (16)–(18) includes only absolute velocities and describes the motion of an underactuated vehicle since two out of three DOF's can be controlled independently, namely the yaw angle and the surge velocity.

4.2.1 Path Following Objective

Assuming that the vehicle is assigned to converge to the line connecting the waypoints WP_k–WP_{k+1}, the along-track and the cross-track error for a given vehicle position (x,y) are given by:

$$\begin{bmatrix} x_e \\ y_e \end{bmatrix} = \mathbf{R}^\top(\gamma_p) \begin{bmatrix} x - x_k \\ y - y_k \end{bmatrix}, \tag{21}$$

where (x_k, y_k) is the position of the k-th waypoint expressed in the NED frame, and the rotation matrix from the inertial frame to the path-fixed reference frame is given by:

$$\mathbf{R}(\gamma_p) = \begin{bmatrix} \cos(\gamma_p) & -\sin(\gamma_p) \\ \sin(\gamma_p) & \cos(\gamma_p) \end{bmatrix} \in SO(2). \tag{22}$$

Moreover,

$$x_e = (x - x_k)\cos(\gamma_p) + (y - y_k)\sin(\gamma_p), \tag{23}$$

$$y_e = -(x - x_k)\sin(\gamma_p) + (y - y_k)\cos(\gamma_p), \tag{24}$$

where γ_p is the horizontal path-tangential angle:

$$\gamma_p = \mathrm{atan2}(y_{k+1} - y_k, x_{k+1} - x_k), \tag{25}$$

where the two-argument function atan2 is a generalization of the $\arctan(y/x)$ that takes into account the signs of both x and y in order to determine the quadrant of the result, hence making it possible to distinguish between diametrically opposite directions. Finally, the associated control objective for horizontal plane straight-line path-following is:

$$\lim_{t \to +\infty} y_e(t) = 0. \tag{26}$$

Note that the along-track error x_e does not need to be minimized in a path-following scenario, the contrary is true for applications that impose temporal constraints.

4.2.2 Horizontal LOS Guidance Law

Figure 4 depicts the geometry of the LOS guidance and some of the main variables that are involved in the problem. Before moving on it is useful to mention that the LOS vector is often defined differently in marine applications compared to the definition adopted by the aircraft and missile communities. According to the definition in [42], the LOS is the line that starts at the reference point (that is, the aircraft or the missile) and passes through the objective of the guidance (i.e the target). On the other hand, in marine guidance applications the LOS vector starts at the vessel and passes through a point $\mathbf{p}(x_{\mathrm{los}}, y_{\mathrm{los}})$ which is located on the path-tangential line at a lookahead distance $\Delta_h > 0$ ahead of the direct projection of the vessel's position $\mathbf{p}(x,y)$ on to the path. The latter definition seems to be more congruent with

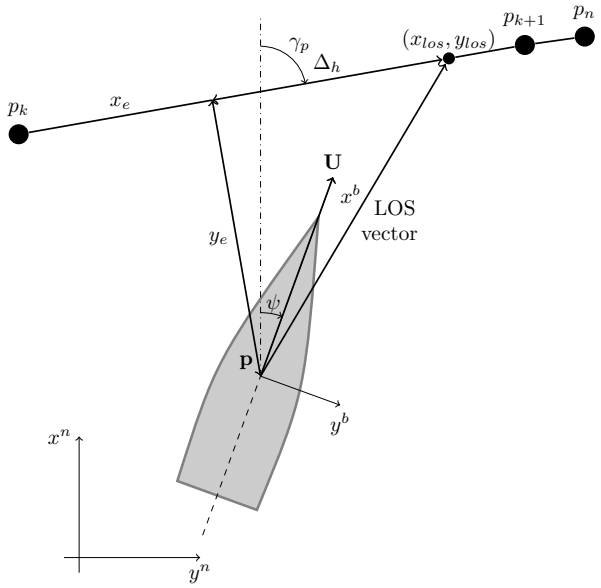

Fig. 4 Line-of-sight guidance geometry for straight lines in the *xy* plane. Here the sideslip angle is equal to zero.

the path-following task and, as a consequence, in this paper the lookahead-based steering method will be considered. Depending on the lookahead distance value, the maneuvering characteristics of the vehicle can vary significantly. More specifically, a low Δ_h value will induce more aggressive steering compared to a larger value. For this reason, algorithms proposing a time-varying Δ_h have been implemented in the past in order to obtain a more flexible behavior, see for instance [34], [32] and [27]. However, in this paper we will consider the different guidance laws with a constant Δ_h in order to reduce the overall complexity of the problem and be able to compare their performance more reliably. The lookahead-based guidance law is given by (see [6]):

$$\psi_d = \gamma_p + \arctan\left(\frac{-y_e}{\Delta_h}\right). \tag{27}$$

In the presence of external disturbances, or during turns, the heading angle ψ_d and the course angle χ_d are not aligned anymore and are related in the following way:

$$\chi_d = \psi_d + \beta, \tag{28}$$

and therefore the desired heading angle is:

$$\psi_d = \gamma_p + \arctan\left(\frac{-y_e}{\Delta_h}\right) - \beta. \tag{29}$$

By differentiating (24) with respect to time we get:

$$\begin{aligned}\dot{y}_e =& -\dot{x}\sin(\gamma_p)+\dot{y}\cos(\gamma_p),\\ =& -(u\cos(\psi)-v\sin(\psi))\sin(\gamma_p)\\ &+(u\sin(\psi)+v\cos(\psi))\cos(\gamma_p),\\ =& u\sin(\psi-\gamma_p)+v\cos(\psi-\gamma_p),\end{aligned} \tag{30}$$

and by transforming (62) in amplitude-phase form we get:

$$\begin{aligned}\dot{y}_e &= \sqrt{u^2+v^2}\sin(\psi-\gamma_p+\beta),\\ &= U_h\sin(\psi-\gamma_p+\beta),\end{aligned} \tag{31}$$

where

$$\beta = \text{atan2}(v,u), \tag{32}$$

which is equal to the orientation of the vehicle's velocity vector U_h with respect to the body-fixed frame. In other words, (32) is the angle between the vehicle's velocity orientation and the vehicle's heading. This is the commonly known as sideslip, or drift, angle.

Proposition 1. *Under the assumption that the desired heading is perfectly tracked such that $\psi = \psi_d$, the system* (31) *has a κ-exponentially stable equilibrium point at $y_e = 0$ if the desired heading angle is given by* (29)*.*

Proof. If we assume that the desired heading is perfectly tracked at all times and choose the desired heading angle as in (29), the derivative of the cross-track error becomes:

$$\dot{y}_e = U_h\frac{-y_e}{\sqrt{\Delta_h^2+y_e^2}}. \tag{33}$$

The Lyapunov Function Candidate (LFC)

$$V_1 = \frac{1}{2}y_e^2, \tag{34}$$

has the time-derivative:

$$\dot{V}_1 = U_h\frac{-y_e^2}{\sqrt{\Delta_h^2+y_e^2}}. \tag{35}$$

which is negative for $U_h > 0$. Hence, the origin $y_e = 0$ is a UGAS equilibrium of the system (33). Moreover, on the ball $D_1 = \{y_e \in R | |y_e| \leq \mu_1\}$, $\mu_1 > 0$, we have that

$$\dot{V}_1 = -\frac{U_h y_e^2}{\sqrt{\mu_1^2+\Delta_h^2}} \leq -k_1 y_e^2, \tag{36}$$

for some $0 < k_1 < U_h/(\sqrt{\mu_1^2 + \Delta_h^2})$, which entails that the origin is a ULES equilibrium. The combination of UGAS and ULES implies global κ-exponential stability, as it was shown in [26].

Discussion regarding the sideslip angle β: It is worth clarifying that the sideslip angle that appears in (31) is not induced by any environmental forces, since in this section they are assumed to be zero. The sideslip angle in the present case occurs due to the nonzero sway velocity during a turn, this is what causes a difference between the orientation ψ (heading angle) of the surge velocity u and the orientation χ (course angle) of the total speed U_h. This is depicted in Fig. 5. When the vehicle is moving forward in an environment without external disturbances (i.e. the vessel following the x^n axis), the total velocity U_h is equal to the surge velocity u and there is no sideslip angle. However, during a turn (i.e the vessel moving on the curved path), a part of the total velocity is transferred into sway velocity and the sideslip angle is nonzero. Consequently, this is the sideslip angle that the current section refers to. In the past there have been proofs of the LOS guidance without including this component of β, see for instance [2]. In that case it was still possible to prove stability because this effect is relatively small (although it can be larger for very agile maneuvering) and the related terms can be modeled as part of the interconnecting term of the cascade structure which was shown to satisfy the growth conditions given in [33]. Ideally, however, incorporating (32) in the desired heading command should increase performance.

Comment regarding the lower speed bound $U_{h,\min}$: It is also important to mention that in order for the proof above to be consistent with stability theory, it is necessary to set a specific positive lower bound $U_{h,\min}$ instead of just assuming that $0 < U_h$. This necessity occurs due to the fact that if the velocity is decreasing in a way such that it converges asymptotically to zero, then it is not possible to conclude that the system (33) converges.

4.3 Vertical-Plane Path Following

This problem is similar to the one presented in Section 4.2 In the case of decoupled vertical plane path-following of underwater vehicles, it is common to assume that the yaw angle $\psi = 0^\circ$, consequently the kinematic equations to be considered are:

$$\dot{x} = u\cos(\theta) - w\sin(\theta), \tag{37}$$

$$\dot{z} = -u\sin(\theta) + w\cos(\theta), \tag{38}$$

$$\dot{\theta} = q. \tag{39}$$

Apparently, for this problem the vertical speed is defined as:

$$U_{\mathrm{v}} := \sqrt{u^2 + w^2} > 0, \tag{40}$$

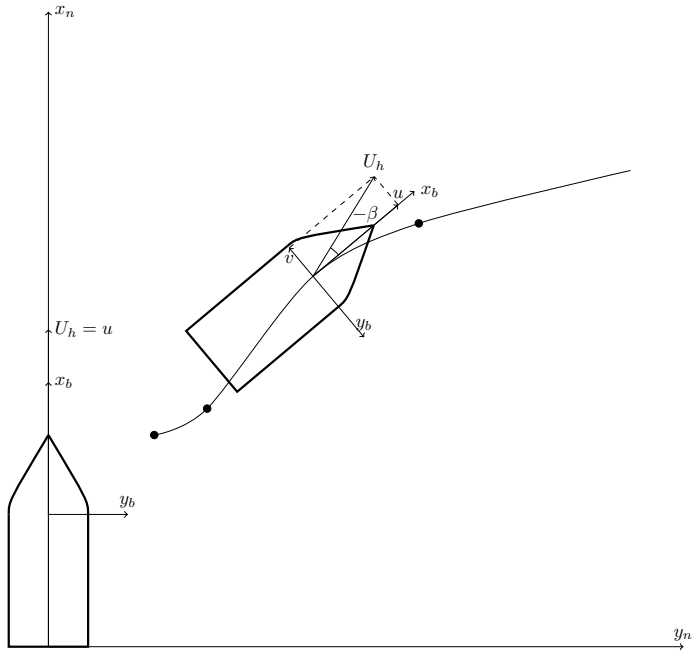

Fig. 5 Sideslip angle during a turn. No external disturbances are present in this case.

and is assumed to be positive and bounded:

$$U_{\text{v,min}} \leq U \leq U_{\text{v,max}}, \;\; 0 < U_{\text{v,min}}. \tag{41}$$

4.3.1 Path Following Objective

Similarly to the case for surface vessels, we assume that the vehicle is supposed to converge to the line connecting the waypoints WP_k–WP_{k+1}, the along-track and the cross-track error for a given vehicle position (x,z) are given by:

$$\begin{bmatrix} x_e \\ z_e \end{bmatrix} = \mathbf{R}^{\top}(\alpha_p) \begin{bmatrix} x - x_k \\ z - z_k \end{bmatrix}, \tag{42}$$

where (x_k, z_k) is the position of the k-th waypoint expressed in the NED frame, and the rotation matrix from the inertial frame to the path-tangential frame is given by:

$$\mathbf{R}(\alpha_p) = \begin{bmatrix} \cos(\alpha_p) & \sin(\alpha_p) \\ -\sin(\alpha_p) & \cos(\alpha_p) \end{bmatrix} \in SO(2). \tag{43}$$

Moreover,

$$x_e = (x - x_k)\cos(\alpha_p) - (z - z_k)\sin(\alpha_p), \tag{44}$$
$$z_e = (x - x_k)\sin(\alpha_p) + (z - z_k)\cos(\alpha_p), \tag{45}$$

where α_p is the vertical path-tangential angle:

$$\alpha_p = \text{atan2}(-(z_{k+1} - z_k), (x_{k+1} - x_k)). \tag{46}$$

Consequently, the associated control objective for vertical plane straight-line path-following is:

$$\lim_{t \to +\infty} z_e(t) = 0. \tag{47}$$

4.3.2 Vertical LOS Guidance Law

The time-derivative of the vertical cross-track error gives:

$$\begin{aligned}
\dot{z}_e =& \dot{x}\sin(\alpha_p) + \dot{z}\cos(\alpha_p), \\
=& -(u\cos(\theta) - w\sin(\theta))\sin(\alpha_p) \\
& -(u\sin(\theta) - w\cos(\theta))\cos(\alpha_p), \\
=& \sqrt{u^2 + w^2}\cos(\theta - \text{atan2}(w,u))\sin(\alpha_p) \\
& -\sqrt{u^2 + w^2}\sin(\theta - \text{atan2}(w,u))\cos(\alpha_p), \\
=& -U_{\text{v}}[\sin(\theta - \alpha)\cos(\alpha_p) - \cos(\theta - \alpha)\sin(\alpha_p)]
\end{aligned} \tag{48}$$

and by transforming (48) according to the common trigonometric property regarding the sinus of a difference of angles:

$$\dot{z}_e = -U_{\text{v}}\sin(\theta - \alpha - \alpha_p), \tag{49}$$

where

$$\alpha = \text{atan2}(w,u) \tag{50}$$

is the commonly known as the angle of attack. Similarly to the horizontal cross-track error case, we assume that the desired pitch angle is perfectly tracked at all times and choose the desired pitch angle as:

$$\theta_d = \alpha_p + \alpha + \arctan\left(\frac{z_e}{\Delta_{\text{v}}}\right), \tag{51}$$

with Δ_{v} denoting the lookahead distance for the vertical-plane LOS.

Proposition 2. *Under the assumption that the desired pitch angle is perfectly tracked such that $\theta = \theta_d$, The system* (49) *has a κ-exponentially stable equilibrium point at $z_e = 0$ if the desired pitch angle is given by* (51).

Proof. Under the assumption of perfect pitch angle tracking, adopting (51) as the desired pitch angle gives the following derivative of the vertical cross-track error:

$$\dot{z}_e = U_{\rm v} \frac{-z_e}{\sqrt{\Delta_{\rm v}^2 + z_e^2}}. \tag{52}$$

The Lyapunov Function Candidate (LFC)

$$V_2 = \frac{1}{2} z_e^2, \tag{53}$$

has the time-derivative:

$$\dot{V}_2 = U_{\rm v} \frac{-z_e^2}{\sqrt{\Delta_{\rm v}^2 + z_e^2}}. \tag{54}$$

which is negative for $U_{\rm v} > 0$. Hence, the origin $z_e = 0$ is a UGAS equilibrium of the system (52). Moreover, on the ball $D_2 = \{z_e \in R | z_e| \leq \mu_2\},\ \mu_2 > 0$, we have that

$$\dot{V}_2 = -\frac{U_{\rm v} z_e^2}{\sqrt{\mu_2^2 + \Delta_{\rm v}^2}} \leq -k_2 z_e^2, \tag{55}$$

for some $0 < k_2 < U_{\rm v}/(\sqrt{\mu_2^2 + \Delta_{\rm v}^2})$, which implies that the origin is a ULES equilibrium point and therefore a κ-exponentially stable equilibrium point.

The same comments and observations mentioned at the end of Section 4.2.2 apply in this case too for both the total speed $U_{\rm v}$ and the angle of attack α.

4.4 Cascade Structure Formed by the Horizontal/Vertical LOS Guidance System and the Heading/Pitch Controller

In the previous sections the assumption of perfectly tracked heading (or pitch, henceforth this clarification will be omitted), such as $\psi = \psi_d$, has been mentioned several times and the stability results have relied on this in order to hold true. Although such an assumption is not congruent with reality, it is not an oversimplification because the guidance system is seen as one of the two systems of a cascaded system. The other subsystem is the heading dynamics, which, apparently, includes the heading controller. Therefore when analyzing the stability of the cascade structure, the theorems and the procedure introduced in [33] are used. Part of this procedure is to analyze the stability of each system independently before taking into account the interconnection between them. Sections 4.2.2 and 4.3.2 dealed with analyzing only the guidance system. The remaining steps depend on the heading autopilot and are outside the scope of this paper, examples can be found in [2] and [27] A depiction of the cascade systems equivalence is shown in Fig. 6.

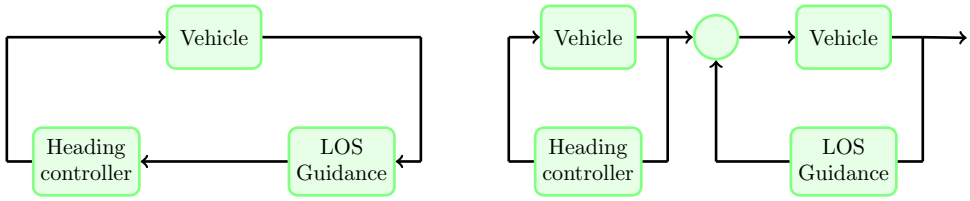

Fig. 6 Cascade system equivalence between the horizontal LOS guidance and the heading controller. The total system can be studied as a cascade structure where the perturbing system (vehicle + heading controller) affects the convergence of the perturbed system (vehicle + LOS guidance) via the heading error dynamics.

5 LOS Guidance Design for 3-D Coupled Motions

5.1 Introduction

This section considers a 3-D motion control scenario where an underwater vehicle is assigned to achieve straight-line path following at a predetermined depth. Contrary to Section 4, the horizontal LOS guidance is now coupled with the vertical motion of the AUV. Hence 5-DOF's are considered and the kinematics is given by (4)–(8) The total speed in this case is:

$$U := \sqrt{u^2 + v^2 + w^2}, \tag{56}$$

where, similarly to the decoupled planar cases of Section 4:

$$U_{\min} \leq U \leq U_{\max}, \;\; 0 < U_{\min}. \tag{57}$$

Comment on the system's structure: The task is to converge to a horizontal straight line at a depth $z = z_d$. Consequently, it is reasonable to consider the two following subsystems in order to solve the problem: a) a depth controller for (6)–(7), and b) a LOS guidance for (4)–(5) and (8). From (6)–(7) we observe that the heave-pitch subsystem is uncoupled with respect to the rest of the states, whereas (4)–(5) and (8) indicates that the horizontal motion is coupled with the vertical plane motion via the pitch angle θ and the heave velocity w. A block diagram of the total system structure can be seen in Fig. 7.

5.2 First Subsystem: Horizontal LOS Guidance Excited by the Heave and Pitch Dynamics

The second subsystem is given by the equations:

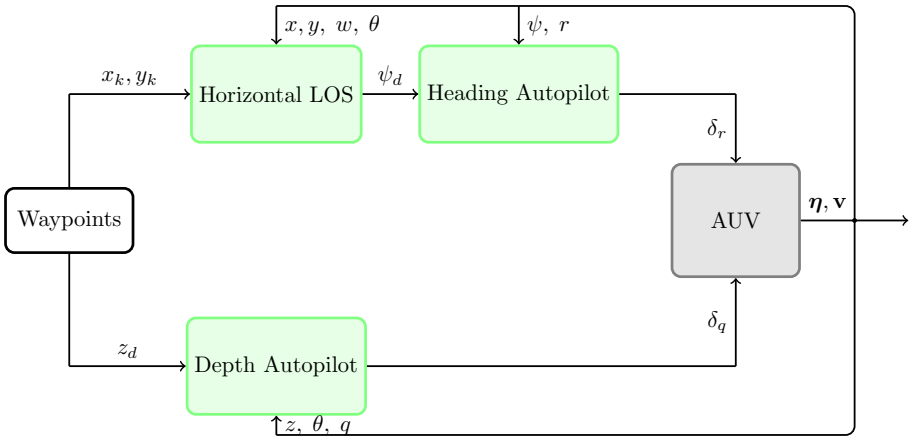

Fig. 7 Block diagram of the 3-D path following scenario. The horizontal plane motion (AUV + LOS guidance) is perturbed by the vertical plane motion (AUV + depth controller). The latter, however, is independent.

$$\dot{x} = u\cos(\psi)\cos(\theta) - v\sin(\psi) + w\cos(\psi)\sin(\theta), \tag{58}$$

$$\dot{y} = u\sin(\psi)\cos(\theta) + v\cos(\psi) + w\sin(\psi)\sin(\theta), \tag{59}$$

$$\dot{\psi} = \frac{1}{\cos(\theta)} r, \quad \cos(\theta) \neq 0. \tag{60}$$

This system is apparently different compared to the horizontal LOS solved in Section 4.2 because the system is now coupled with the depth control system via the pitch angle θ and the heave velocity w. The cross-track error is still given by:

$$y_e = -(x - x_k)\sin(\gamma_p) + (y - y_k)\cos(\gamma_p), \tag{61}$$

however, in this case it propagates differently due to the coupling with θ and w:

$$\begin{aligned} \dot{y}_e &= -\dot{x}\sin(\gamma_p) + \dot{y}\cos(\gamma_p), \\ &= -u\cos(\psi)\cos(\theta)\sin(\gamma_p) + v\sin(\psi)\sin(\gamma_p) \\ &\quad - w\cos(\psi)\sin(\theta)\sin(\gamma_p) + u\sin(\psi)\cos(\theta)\cos(\gamma_p) \\ &\quad + v\cos(\psi)\cos(\gamma_p) + w\sin(\psi)\sin(\theta)\cos(\gamma_p). \end{aligned} \tag{62}$$

Using several trigonometric identities yields:

$$\begin{aligned} \dot{y}_e =& -\cos(\psi)\sin(\gamma_p)[u\cos(\theta) + w\sin(\theta)] \\ &+ \sin(\psi)\cos(\gamma_p)[u\cos(\theta) + w\sin(\theta)] + v\cos(\psi - \gamma_p), \\ =& \sqrt{u^2 + w^2}\cos(\theta - \alpha)[\sin(\psi)\cos(\gamma_p) - \cos(\psi)\sin(\gamma_p)] + v\cos(\psi - \gamma_p), \\ =& U_{\mathrm{v}}\cos(\theta - \alpha)\sin(\psi - \gamma_p) + v\cos(\psi - \gamma_p), \end{aligned}$$

and, finally, we have the compact form:

$$\dot{y}_e = \sqrt{(U_{\mathrm{v}}^2 \cos^2(\theta - \alpha) + v^2)} \sin(\psi - \gamma_p + \beta_{\mathrm{v}}) \tag{63}$$

where:

$$\beta_{\mathrm{v}} = \mathrm{atan2}(v, U_{\mathrm{v}} \cos(\theta - \alpha)). \tag{64}$$

This result shows that the first subsystem (it intervenes here through θ and w) does not prevent the minimization of the horizontal cross-track error as long as the yaw controller can compensate for the generalized sideslip angle β_{v}. This agrees with intuition because if the target line is at a high depth, the horizontal LOS guidance system will probably converge first while the AUV continues to submerge. The desired yaw angle is:

$$\psi_d = \gamma_p - \beta_{\mathrm{v}} + \arctan\left(\frac{-y_e}{\Delta_h}\right). \tag{65}$$

Before proceeding with the theorem and the proof pertinent to the stability of (63), the following assumptions are made:

- *A1:* The desired heading ψ_d is perfectly tracked at all times.
- *A2:* The depth controller ensures that w and θ are bounded states.
- *A3:* The pitch angle satisfies the condition $\theta \neq \pm\frac{\pi}{2}$.

Theorem 1. *The system* (63) *has a* κ*-exponentially stable equilibrium point at* $y_e = 0$ *if all the assumptions A1-A3 are satisfied and the desired heading angle is given by* (65).

Proof. This is similar to the cases proved in Section 4. The Lyapunov Function Candidate (LFC):

$$V_3 = \frac{1}{2} y_e^2, \tag{66}$$

has the time-derivative:

$$\dot{V}_3 = \sqrt{(U_{\mathrm{v}}^2 \cos^2(\theta - \alpha) + v^2)} \frac{-y_e^2}{\sqrt{\Delta_h^2 + y_e^2}}. \tag{67}$$

which is negative. Hence, the origin $y_e = 0$ is a UGAS equilibrium of the system (52). In addition, on the ball $D_3 = \{y_e \in R | y_e| \leq \mu_3\}$, $\mu_3 > 0$, we have that

$$\dot{V}_3 = -\frac{\sqrt{(U_{\mathrm{v}}^2 \cos^2(\theta - \alpha) + v^2)} y_e^2}{\sqrt{\mu_3^2 + \Delta_h^2}} \leq -k_3 y_e^2, \tag{68}$$

for some $0 < k_3 < \sqrt{(U_v^2 \cos^2(\theta - \alpha) + v^2)/(\mu_3^2 + \Delta_h^2)}$, which implies that the origin is a ULES equilibrium point and therefore a κ-exponentially stable equilibrium point.

5.3 Second Subsystem: Depth Control

This section discusses two popular approaches when it comes to depth control of AUVs, namely, PID control and sliding mode control. Note that several other methodologies have been studied in the past, such as adaptive linear controllers [28], model predictive controllers [38] and H_∞ control [20], [29], [35]. More detailed information on similar control techniques for AUVs can be found in [25]. At the end of the section we discuss the possibility of the depth reference trajectories being generated by a vertical LOS guidance algorithm. Although such a concept can be characterized as redundant when the overall task of the depth controller is to achieve setpoint regulation, it constitutes an important step toward an even more general path-following scenario where the task is to converge to any straight line in space (i.e. $\gamma_p,\ \alpha_p \neq 0$), hence a time-varying depth reference signal is required.

5.3.1 Conventional PID Controllers

Controlling depth using PID controllers is a common approach that has been reported in the literature, see for instance [23], [41], [31]. Usually, this approach employs a linearized model for the pitch dynamics and conventional PID controllers are tuned properly in order to stabilize the system. As it is always the case with linearized systems, the approach might fail for large pitch angles, or time-varying velocity. However, if the linearization assumptions are satisfied then the PID controller will result theoretically in a GES equilibrium point. Experimental tests using PID controllers for depth control have reported satisfactory performance and this fact in combination with their simplicity makes them a more attractive approach compared to a more complicated one like, for instance, H_∞ control [25].

5.3.2 Sliding Mode Controllers

Depth control using sliding modes is also a methodology that has been implemented extensively in the past, an early reference is that of [13], in-water tests were reported in [22], also a well-known approach was the one presented in [21]. This controller is based on the concept of the sliding surface to increase robustness and its goal is to provide good performance even under the presence of modeling uncertainties and environmental disturbances. A sliding mode controller demonstrates better performance and is faster compared to a PID controller, but the downside is that it is more complicated and requires a complete model. An example of a pitch and depth au-

topilot for underwater vehicles based on sliding mode control can be found in [16, pp. 526–528].

5.3.3 Vertical LOS for Depth Control

Adopting vertical LOS coupled with horizontal LOS is the next reasonable step in order to achieve path following for any straight path in space, with the exception of $\alpha_p \pm \pi/2$ due to the singularity of the Euler angle representation. It is possible to avoid this singularity by using quaternions. Due to the fact that the kinematics (6)–(7) is uncoupled, the analysis from Section 4.3 still holds. Therefore, combining (63) and (51) and using the property

$$\cos(\arctan(x)) = 1/(\sqrt{1+x^2}), \tag{69}$$

gives:

$$\dot{y}_e = \frac{U_{\mathrm{v}}\Delta_{\mathrm{v}}}{\sqrt{\Delta_{\mathrm{v}}^2 + z_e^2}} \sin(\psi - \gamma_p) + v\cos(\psi - \gamma_p), \tag{70}$$

and finally we get the compact form:

$$\dot{y}_e = \sqrt{\left(\frac{U_{\mathrm{v}}^2\Delta_{\mathrm{v}}^2}{\Delta_{\mathrm{v}}^2 + z_e^2} + v^2\right)} \sin(\psi - \gamma_p + \beta_{\mathrm{v}}), \tag{71}$$

with

$$\beta_{\mathrm{v}} = \mathrm{atan2}\left(v, \frac{U_{\mathrm{v}}\Delta_{\mathrm{v}}}{\sqrt{\Delta_{\mathrm{v}}^2 + z_e^2}}\right). \tag{72}$$

As expected, (71) shows that the horizontal cross-track error is now a function of the vertical cross-track error as well. Note, however, that z_e does not prevent y_e from converging because the stability result for the vertical LOS guarantees that z_e is bounded and has a κ-exponentially stable equilibrium point at $z_e = 0$. Eq. (72) shows an generalized formulation of the sideslip angle. Similarly to the 2-D sideslip angle case, this has an effect if the sway motion is nonzero, i.e. on a turn. Apparently, the system (71) is stabilized with a heading command:

$$\psi_d = \gamma_p - \beta_{\mathrm{v}} + \arctan\left(\frac{-y_e}{\Delta_h}\right). \tag{73}$$

This can be shown similarly to the previous proofs, for a LFC:

$$V_4 = \frac{1}{2}y_e^2, \tag{74}$$

we derivate V_4 w.r.t time and use (73) as the desired heading command. The final result is:

$$\dot{V}_4 = -\sqrt{\left(\frac{U_{\mathrm{v}}^2 \Delta_{\mathrm{v}}^2}{\Delta_{\mathrm{v}}^2 + z_e^2} + v^2\right)} \left(\frac{y_e^2}{\Delta_h^2 + y_e^2}\right). \tag{75}$$

6 LOS Guidance Under the Influence of Sea Currents

6.1 Introduction

Section 4 considered path-following in 3-DOF under the assumption that no external disturbances affect the vehicle. However this is rarely, if ever, true in real life applications. In practice there is always influence due to the waves, wind and ocean currents. The natural outcome then is that the LOS guidance will fail to succeed in achieving the motion control objective. More specifically, when the desired path is a straight line, these (hypothetically constant, or slow time-varying) forces will result in a constant cross-track error from the target line. The magnitude of this error depends on the magnitude of the total external force, as well as the force's orientation with respect to the target line. It is common practice in control systems to add an integrator to the system in order to eliminate constant offsets and, naturally, this has been implemented to LOS guidance in the past. The idea is to accumulate the error with an integral term and use it to correct the heading (or pitch) reference trajectories until the error has been eliminated. As a consequence, when the vehicle eventually converges on the target line, its heading will not be equal with the course angle. In other words, a sideslip angle is necessary in order for the vehicle to converge to and follow the path. In connection with the discussion on the sideslip angle (32) due to turning in Section 4.2.2, the sideslip angle because of the external forces is given by:

$$\beta_r = \mathrm{atan2}(v_r, u_r), \tag{76}$$

see also Fig. 8. In the rest of this section, two integral LOS guidance laws pertaining to marine vehicles are revised. Finally, it is also shown how course control (whenever applicable) circumvents this problem.

6.2 Conventional Integral LOS Guidance

Following [6], by rewriting (29) as

$$\psi_d = \gamma_p + \underbrace{\arctan(-K_p y_e)}_{\psi_r} - \beta,\ K_p = (1/\Delta), \tag{77}$$

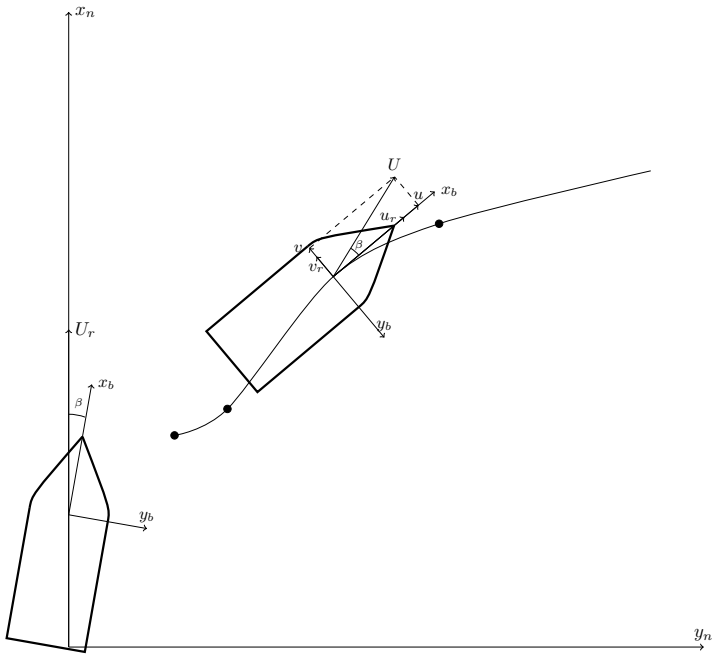

Fig. 8 Sideslip angle, with a current coming from the east, hence affecting the velocity components.

we observe that the lookahead-based steering law has the same form as a saturated proportional control law, effectively mapping $y_e \in R$ into $\psi_r(y_e) \in (-\pi/2, \pi/2)$. Following the same line of reasoning, it is straightforward to add integral action in order to compensate for the cross-track error caused by a constant disturbance:

$$\psi_d = \gamma_p + \arctan\left(-K_p y_e - K_i \int_{t_0}^{t} y_e d\tau\right). \tag{78}$$

where $K_i > 0$ denotes the integral gain. As is usually the case with integral control action, careful design is necessary so as to avoid undesired effects such as wind-up and overshooting. Wind-up refers to the case where the integral term increases to large values and, as a consequence, has negative effects on the system's performance, such as very long convergence time and overshooting. Suggested methodologies pertaining to avoiding such phenomena can be found in [12], [8]. Equation (78) can be rewritten as follows

$$\psi_d = \gamma_p + \arctan\left(-K_p y_e - K_i y_{\text{int}}\right), \tag{79}$$

$$\dot{y}_{\text{int}} = y_e. \tag{80}$$

6.3 Integral LOS Guidance

In [1] the authors followed a different approach and presented the following modified LOS guidance law with integral action:

$$\psi_d = \gamma_p - \arctan(K_p y_e + K_i y_{\text{int}}) \tag{81}$$

$$\dot{y}_{\text{int}} = \frac{y_e \Delta}{\Delta^2 + (y_e + \kappa y_{\text{int}})^2}, \tag{82}$$

where $K_p = (1/\Delta)$, $K_i = K_p \kappa$ and $\kappa > 0$ is a design parameter. Equation (82) has been designed in a way such that the influence of the integrator diminishes when the cross-track error increases, hence the wind-up risk is reduced. The authors focus on marine surface vessels and they pair the proposed guidance law (81)–(82) with a set of adaptive tracking controllers. After a long and extensive analysis they show that, after explicit bounds on the parameters of the guidance law have been satisfied, their proposed strategy results in globally asymptotic path following. The analysis in [1] was based on the 3-DOF kinematic model (16)–(18) with absolute velocities. In [9] the authors presented a proof of the same integral LOS guidance law using the relative velocity kinematics (9)–(10) and (13) (with $\theta = 0$) and showed that this simplifies the overall analysis and results in less complicated controllers. Fig. 9 compares the performance between the conventional integral LOS and the method developed by Børhaug et al.

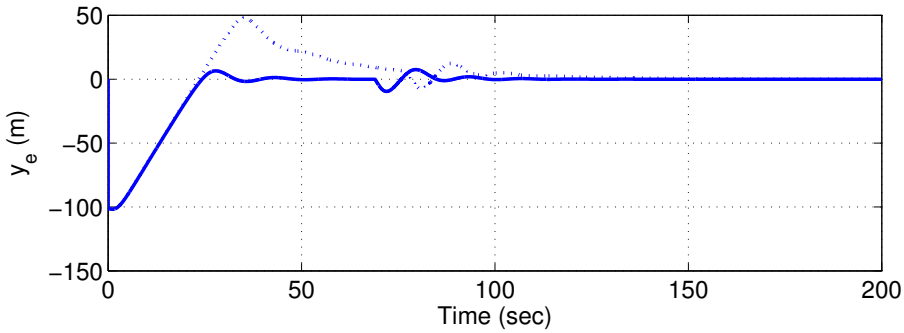

Fig. 9 Cross-track error comparison between the conventional integral LOS (dotted line) and the integral LOS proposed by Børhaug et al. (solid line).

6.4 LOS Guidance using Course Control

In a path-following operation of a surface vehicle it is natural to assume that GNSS (Global Navigation Satellite System) measurements are available, otherwise it is not possible to compute the cross-track error, for instance. Consequently, it is feasible to get absolute velocity measurements that can be used to control the course angle χ of the ship. Especially in the case of devices using GNNS Doppler data, the achievable accuracy can be very high, as it is reported in [10]. The ability to control χ allows to tackle the problem in a different way by rewriting the cross-track error (31) as

$$\dot{y}_e = U \sin(\chi_d - \gamma_p), \tag{83}$$

which, similarly to the proof in Section 4, can be easily shown to have a κ-exponentially stable equilibrium point at $y_e = 0$ by choosing the desired course angle as:

$$\chi_d = \gamma_p + \arctan\left(\frac{-y_e}{\Delta}\right). \tag{84}$$

Interestingly, it can be concluded by comparing (84) with (81) that, by controlling the course angle instead of the heading angle, the integral term is not necessary anymore. This is a natural outcome of expressing the cross-track error in the form (31) because in that way it becomes entirely known how the sideslip angle affects y_e. As a result, the necessity to deal with the current effect uncertainty is circumvented because the law (84) attempts to lead the overall velocity vector orientation to the right value, hence there is no need for an extra state that will accumulate the cross-track error so as to compensate for the heading control deviation from that orientation. It is worth noting that in previous works the desired course command fed into the course controller included integral action as well, see for instance [36] and [7]. In practice, however, it will probably still be useful to include integral action because there are always model uncertainties and other unknown factors present that have to be compensated for. Fig. 10 compares the performance between the course control case and the integral LOS guidance law developed by Børhaug et al. As it was expected, the fact that there is no uncertainty from the beginning in the course control method leads to better results.

7 Conclusions

This paper has given an overview of the LOS guidance law for marine vehicles. Proofs in 3-DOF for horizontal and vertical plane navigation incorporating the sideslip angle and the angle of attack were given. Then, the more general task of converging to a horizontal line at a predetermined depth underwater was studied. The effect of constant environmental forces were discussed and two methods from the literature were revised and compared. Moreover, it was shown that controlling the course instead of the yaw angle removes all the uncertainty and leads to even

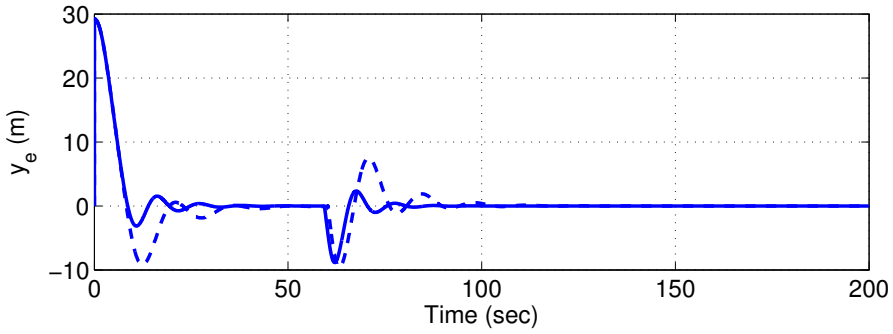

Fig. 10 Cross-track error comparison between the course control case (solid line) and the integral LOS proposed by Børhaug et al. (dashed line).

better performance. The cascade structure between the guidance system and the heading dynamics was discussed. The importance of choosing a suitable path depending on the application was stressed and, in addition, a section proposing path evaluation criteria was presented.

8 Acknowledgments

The first author wishes to acknowledge useful discussions with Andreas Reason Dahl and Dr. Morten Breivik regarding the path evaluation criteria. This work was supported by the Centre for Ships and Ocean Structures, the Centre for Autonomous Marine Operations and Systems, NTNU, and the Norwegian Research Council.

References

1. Børhaug, E., Pavlov, A., Pettersen, K.Y.: Integral LOS control for path following of underactuated marine surface vessels in the presence of constant ocean currents. In: 47th IEEE Conference on Decision and Control, pp. 4984–4991. Cancun, Mexico (2008)
2. Børhaug, E., Pettersen, K.Y.: Cross-track control for underactuated autonomous vehicles. In: Proceedings of the 44th IEEE Conference on Decision and Control, and the European Control Conference, pp. 602–608. Seville, Spain (2005)
3. Breivik, M.: Topics in guided motion control of marine vehicles. Ph.D. thesis, Norwegian University of Science and Technology (2010)
4. Breivik, M., Fossen, T.I.: Path following for marine surface vessels. In: Proceedings of the OTO'04, pp. 2282–2289. Kobe, Japan (2004)
5. Breivik, M., Fossen, T.I.: Principles of guidance-based path following in 2D and 3D. In: Proceedings of the 44th IEEE Conference on Decision and Control, and the European Control Conference, pp. 627–634. Seville, Spain (2005)

6. Breivik, M., Fossen, T.I.: Guidance laws for autonomous underwater vehicles, chap. 4, pp. 51–76. INTECH Education and Publishing (2009)
7. Breivik, M., Hovstein, V.E., Fossen, T.I.: Straight-line target tracking for unmanned surface vehicles. Modeling, Identification and Control **29**(4), 131–149 (2008)
8. Burger, M.: Disturbance rejection using conditional integrators. Ph.D. thesis, Norwegian University of Science and Technology (2011)
9. Caharija, W., Candeloro, M., Pettersen, K.Y., Sørensen, A.J.: Relative velocity control and integral LOS for path following of underactuated surface vessels. In: 9th IFAC Conference on Manoeuvring and Control of Marine Craft. Arenzano, Italy (2012)
10. Chalko, T.J.: High accuracy speed measurement using GPS (Global Positioning System). Scientific Engineering Research P/L (2002)
11. Dahl, A.R.: Overview and evaluation of path planning and guidance algorithms. Tech. rep., Department of Engineering Cybernetics, NTNU (2012)
12. Davidson, M., Bahl, V., Moore, K.L.: Spatial integration for a nonlinear path tracking control law. In: Proceedings of the 2002 American Control Conference., pp. 4291–4296. IEEE (2002)
13. Dougherty, F., Woolweaver, G.: At-sea testing of an unmanned underwater vehicle flight control system. In: Proceedings of the (1990) Symposium on Autonomous Underwater Vehicle Technology, pp. 65–73. IEEE (1990)
14. Dubins, L.E.: On curves of minimal length with a constraint on average curvature, and with prescribed initial and terminal positions and tangents. American Journal of Mathematics **79**(3), 497–516 (1957)
15. Farouki, R.T., Sakkalis, T.: Pythagorean hodographs. IBM Journal of Research and Development **34**(5), 736–752 (1990)
16. Fossen, T.I.: Handbook of Marine Craft Hydrodynamics and Motion Control. John Wiley and Sons Ltd. (2011)
17. Fossen, T.I.: How to incorporate wind, waves and ocean currents in the marine craft equations of motion. In: 9th IFAC Conference on Manoeuvring and Control of Marine Craft. Arenzano, Italy (2012)
18. Fossen, T.I., Breivik, M., Skjetne, R.: Line-of-sight path following of underactuated marine craft. Proceedings of the 6th IFAC MCMC, Girona, Spain pp. 244–249 (2003)
19. Fritsch, F.N., Carlson, R.E.: Monotone piecewise cubic interpolation. SIAM Journal on Numerical Analysis **17**(2), 238–246 (1980)
20. Fryxell, D., Oliveira, P., Pascoal, A., Silvestre, C.: Integrated design of navigation, guidance and control systems for unmanned underwater vehicles. In: Proceedings OCEANS '94, vol. 3, pp. III–105. IEEE (1994)
21. Healey, A.J., Lienard, D.: Multivariable sliding mode control for autonomous diving and steering of unmanned underwater vehicles. IEEE Journal of Oceanic Engineering **18**(3), 327–339 (1993)
22. Hills, S.J., Yoerger, D.R.: A nonlinear sliding mode autopilot for unmanned undersea vehicles. In: Proceedings OCEANS'94., vol. 3, pp. III–93. IEEE (1994)
23. Jalving, B.: The NDRE-AUV flight control system. IEEE Journal of Oceanic Engineering **19**(4), 497–501 (1994)
24. LaValle, S.M.: Planning algorithms. Cambridge university press (2006)
25. Lea, R.K., Allen, R., Merry, S.L.: A comparative study of control techniques for an underwater flight vehicle. International Journal of Systems Science **30**(9), 947–964 (1999)
26. Lefeber, E.: Tracking control of nonlinear mechanical systems. Ph.D. thesis, University of Twente (2000)
27. Lekkas, A.M., Fossen, T.I.: A time-varying lookahead distance guidance law for path following. In: 9th IFAC Conference on Manoeuvring and Control of Marine Craft. Arenzano, Italy (2012)
28. Li, J.H., Lee, P.M.: Design of an adaptive nonlinear controller for depth control of an autonomous underwater vehicle. Ocean engineering **32**(17), 2165–2181 (2005)
29. Liceaga-Castro, E., van der Molen, G.M.: Submarine H_∞ depth control under wave disturbances. IEEE Transactions on Control Systems Technology **3**(3), 338–346 (1995)

30. Lipschutz, M.M.: Differential Geometry. McGraw-Hill (1969)
31. McEwen, R., Streitlien, K.: Modeling and control of a variable-length AUV. Proc 12th UUST (2001)
32. Oh, S.R., Sun, J.: Path following of underactuated marine surface vessels using line-of-sight based model predictive control. Ocean Engineering **37**(2-3), 289–295 (2010)
33. Panteley, E., Loría, A.: On global uniform asymptotic stability of nonlinear time-varying systems in cascade. Systems & Control Letters **33**(2), 131–138 (1998)
34. Pavlov, A., Nordahl, H., Breivik, M.: MPC-based optimal path following for underactuated vessels. In: 8th IFAC International Conference on Manoeuvring and Control of Marine Craft, pp. 340–345. Guaruja, Brazil (2009)
35. Silvestre, C., Pascoal, A., Healey, A.J.: AUV control under wave disturbances. In: International Symposium on Unmanned Untethered Submersible Technology, pp. 228–239. University of New Hampshire-Marine Systems (1997)
36. Skejic, R., Breivik, M., Berg, T.E.: Investigating ship maneuvers around a floating structure under the influence of a uniform current in deep and calm water. In: Second International Conference on Ship Manoeuvring in Shallow and Confined Water: Ship to Ship Interaction, pp. 339 – 350 (2011)
37. Sørdalen, O.J., Egeland, O.: Exponential stabilization of nonholonomic chained systems. IEEE Transactions on Automatic Control **40**(1), 35–49 (1995)
38. Steenson, L.V., Phillips, A.B., Turnock, S.R., Furlong, M.E., Rogers, E.: Effect of measurement noise on the performance of a depth and pitch controller using the model predictive control method. In: Autonomous Underwater Vehicles (AUV), 2012 IEEE/OES, pp. 1–8. IEEE (2012)
39. Techy, L., Woolsey, C.A.: Minimum-time path planning for unmanned aerial vehicles in steady uniform winds. Journal of guidance, control, and dynamics **32**(6), 1736–1746 (2009)
40. Tsourdos, A., White, B., Shanmugavel, M.: Cooperative path planning of unmanned aerial vehicles. Wiley Online Library (2011)
41. Williams, S.B., Newman, P., Dissanayake, G., Rosenblatt, J., Durrant-Whyte, H.: A decoupled, distributed AUV control architecture. In: International Symposium on Robotics, vol. 31, pp. 246–251. unknown (2000)
42. Yanushevsky, R.: Guidance of Unmanned Aerial Vehicles. CRC Press (2011)